



HAL
open science

Loop Current Variability as Trigger of Coherent Gulf Stream Transport Anomalies

Joël J.-M. Hirschi, Eleanor Frajka-Williams, Adam T. Blaker, Bablu Sinha, Andrew C. Coward, Pat Hyder, Arne Biastoch, Claus W. Böning, Bernard Barnier, Thierry Penduff, et al.

► **To cite this version:**

Joël J.-M. Hirschi, Eleanor Frajka-Williams, Adam T. Blaker, Bablu Sinha, Andrew C. Coward, et al.. Loop Current Variability as Trigger of Coherent Gulf Stream Transport Anomalies. *Journal of Physical Oceanography*, 2019, 49 (8), pp.2115-2132. 10.1175/JPO-D-18-0236.1 . hal-02281908

HAL Id: hal-02281908

<https://hal.sorbonne-universite.fr/hal-02281908>

Submitted on 9 Sep 2019

HAL is a multi-disciplinary open access archive for the deposit and dissemination of scientific research documents, whether they are published or not. The documents may come from teaching and research institutions in France or abroad, or from public or private research centers.

L'archive ouverte pluridisciplinaire **HAL**, est destinée au dépôt et à la diffusion de documents scientifiques de niveau recherche, publiés ou non, émanant des établissements d'enseignement et de recherche français ou étrangers, des laboratoires publics ou privés.

Loop Current Variability as Trigger of Coherent Gulf Stream Transport Anomalies

JOËL J.-M. HIRSCHI,^a ELEANOR FRAJKA-WILLIAMS,^a ADAM T. BLAKER,^a BABLU SINHA,^a
ANDREW COWARD,^a PAT HYDER,^b ARNE BIASTOCH,^c CLAUS BÖNING,^c BERNARD BARNIER,^d
THIERRY PENDUFF,^d IXETL GARCIA,^d FILIPPA FRANSNER,^e AND GURVAN MADEC^f

^a National Oceanography Centre, Southampton, United Kingdom

^b Met Office, Exeter, United Kingdom

^c Helmholtz Centre for Ocean Research, Kiel, Germany

^d Université Grenoble Alpes, CNRS, IRD, Grenoble INP, IGE, Grenoble, France

^e Geophysical Institute, University of Bergen, and Bjerknes Centre for Climate Research, Bergen, Norway

^f LOCEAN (CNRS/IRD/UPMC/MNHN) Institut Pierre et Simon Laplace, Paris, France

(Manuscript received 17 November 2018, in final form 8 May 2019)

ABSTRACT

Satellite observations and output from a high-resolution ocean model are used to investigate how the Loop Current in the Gulf of Mexico affects the Gulf Stream transport through the Florida Straits. We find that the expansion (contraction) of the Loop Current leads to lower (higher) transports through the Straits of Florida. The associated surface velocity anomalies are coherent from the southwestern tip of Florida to Cape Hatteras. A simple continuity-based argument can be used to explain the link between the Loop Current and the downstream Gulf Stream transport: as the Loop Current lengthens (shortens) its path in the Gulf of Mexico, the flow out of the Gulf decreases (increases). Anomalies in the surface velocity field are first seen to the southwest of Florida and within 4 weeks propagate through the Florida Straits up to Cape Hatteras and into the Gulf Stream Extension. In both the observations and the model this propagation can be seen as pulses in the surface velocities. We estimate that the Loop Current variability can be linked to a variability of several Sverdrups ($1\text{ Sv} = 10^6\text{ m}^3\text{ s}^{-1}$) through the Florida Straits. The exact timing of the Loop Current variability is largely unpredictable beyond a few weeks and its variability is therefore likely a major contributor to the chaotic/intrinsic variability of the Gulf Stream. However, the time lag between the Loop Current and the flow downstream of the Gulf of Mexico means that if a lengthening/shortening of the Loop Current is observed this introduces some predictability in the downstream flow for a few weeks.

1. Introduction

The Gulf Stream is a vigorous, warm surface western boundary current that forms the western branch of the Atlantic subtropical gyre. Its westward intensification is a direct consequence of Earth's rotation and of the resulting Coriolis force. On a sphere the Coriolis force depends on the latitude (vanishing at the equator;

maximum at the poles) and it is this latitude dependence that leads to the westward intensified ocean circulation found along the western margins of the ocean basins (Stommel 1948). Of all western boundary currents the Gulf Stream is the best observed. In the Florida Straits it has been measured almost continuously since 1982 based on the voltage induced in submerged telecommunication cables (Larsen and Smith 1992; Baringer and Larsen 2001; DiNezio et al. 2009). On average the Gulf Stream transports about 31 Sv ($1\text{ Sv} \equiv 10^6\text{ m}^3\text{ s}^{-1}$) through the Florida Straits (Baringer and Larsen 2001; DiNezio et al. 2009). At Cape Hatteras the Gulf Stream separates from the U.S. coast and flows eastward into the open Atlantic as the Gulf Stream Extension. Part of this current recirculates south in the upper ocean forming the eastern branch of the Subtropical Gyre and part of it flows northward toward the subpolar North

Denotes content that is immediately available upon publication as open access.

Supplemental information related to this paper is available at the Journals Online website: <https://doi.org/10.1175/JPO-D-18-0236.s1>.

Corresponding author: Joël J.-M. Hirschi, joel.hirschi@noc.ac.uk

DOI: 10.1175/JPO-D-18-0236.1

© 2019 American Meteorological Society. For information regarding reuse of this content and general copyright information, consult the AMS Copyright Policy (www.ametsoc.org/PUBSReuseLicenses).

Atlantic as the North Atlantic Current (NAC). The Gulf Stream constitutes a large fraction of the northward flowing surface branch of the Atlantic meridional overturning circulation (AMOC; [Cunningham et al. 2007](#); [McCarthy et al. 2012](#); [Smeed et al. 2014](#)).

As part of the AMOC the Gulf Stream affects climate and weather in the North Atlantic region and contributes to the net northward heat transport associated with the AMOC (e.g., [Johns et al. 2011](#)). The cable measurements suggest that the Gulf Stream transport through the Florida Straits has been largely stable during the last few decades. However, the transport is characterized by a large sub- to interannual variability. The majority of studies into the variability of the Gulf Stream transport have addressed the problem in terms of whether the temporal transport variability can be explained as a response to variability in the atmospheric forcing (e.g., [Anderson and Corry 1985](#); [DiNezio et al. 2009](#); [Meinen et al. 2010](#); [Atkinson et al. 2010](#); [Sanchez-Franks et al. 2016](#)). However, no approach can explain the full variability seen in the Gulf Stream transport. Arguments based on the wind stress/wind stress curl (e.g., [Anderson and Corry 1985](#); [Atkinson et al. 2010](#); [Sanchez-Franks et al. 2016](#)) argue that winds occurring either up or downstream of the Florida Straits are a main source of variability. However, it is also clear that the transport variability cannot be explained from the surface forcing alone. An example of this is the seasonal cycle seen in the Florida Straits transport ([Niiler and Richardson 1973](#)). The Florida Straits time series extending back to 1982 shows that this seasonal cycle is subject to a large interannual variability. In some years it is clearly defined, whereas during other years/periods the seasonal cycle is hardly visible. Seasonal variability in the large-scale wind is thought to explain the seasonal cycle, but the wind has a seasonal cycle with comparatively little interannual variability and it is clear that factors other than wind determine the Gulf Stream variability on short, that is, subannual to annual time scales. In particular the Gulf Stream is subject to a large chaotic/intrinsic variability ([Lin et al. 2010](#); [Atkinson et al. 2010](#); [Mildner et al. 2013](#)). Subjecting a model to the same atmospheric variability but starting from different initial conditions leads to different timings in the transports with low correlations between the different model realizations ([Atkinson et al. 2010](#)). The presence of chaotic (intrinsic) variability in the ocean has been studied before (e.g., [Biastoch et al. 2008](#); [Penduff et al. 2011](#); [Hirschi et al. 2013](#); [Grégorio et al. 2015](#); [Leroux et al. 2018](#)) but the emphasis of these studies was on variability of the sea surface height (SSH) or the AMOC and not on boundary currents. While the impact of the largely chaotic ocean eddies on the Gulf Stream

transport is far from fully understood previous studies suggest that Loop Current eddies account for a sizeable fraction of the total variability in the Gulf Stream transport ([Lin et al. 2010](#); [Mildner et al. 2013](#))—in particular that certain stages of the Loop Current coincide with minima in the volume transport through the Straits of Florida. The suggested mechanisms leading to reduced transport through the Florida Straits are either density and bottom pressure anomalies in response to an interaction between the Loop Current and the bottom topography between Florida and Cuba ([Lin et al. 2010](#)) or the partial blockage of transport through the Yucatan Channel (and hence at the outflow of the Gulf of Mexico through the Florida Straits) by Loop Current rings ([Mildner et al. 2013](#)).

In this study we will show that there is a third, perhaps even simpler mechanism through which the Loop Current evolution can influence the variability of the volume transport through the Straits of Florida. Our results are based on a global high-resolution ($1/12^\circ$) ocean model and on satellite altimetry and concentrate on the coherent current made up of the Yucatan Current, the Loop Current, the Florida Current, and the Gulf Stream. In the following we will refer to this “river-like” part of the current as the “Gulf Stream.” We show that variability on seasonal to interannual time scales exhibits a large spatial coherence along the U.S. coastline and that the temporal evolution of the Loop Current is central to the variability found farther downstream in the Straits of Florida and along the eastern U.S. coast. We also show that the Loop Current is the trigger of pulses in the Gulf Stream transport which propagate from the Gulf of Mexico to Cape Hatteras in about 1 month.

2. Data and method

The data used in this study consists of output from a high-resolution global ocean model, geostrophic ocean surface velocities calculated from satellite altimetry and time series for the Gulf Stream transport obtained from cable measurements across the Florida Straits. For both the Florida Straits transport and surface velocities there are good quality observational data: the Florida Straits transport has been (almost) continuously observed since 1982 and surface velocities can be inferred from satellite altimetry since 1993. These quantities can also easily be compared to results obtained in numerical ocean models (e.g., [Marzocchi et al. 2015](#)). The models then can be used to provide a more complete picture of the circulation as they can simulate the large-scale three-dimensional flow field at high resolution—something which cannot yet be obtained from observations.

The numerical model used in this study is the Nucleus for European Modeling of the Ocean (NEMO; Madec 2008). NEMO simulates the global ocean circulation and uses the quasi-isotropic tripolar ORCA grid (Madec and Imbard 1996) with a horizontal resolution of $1/12^\circ$. To avoid a singularity at the North Pole the ORCA grid has two poles in the Northern Hemisphere centered on northern Russia and northern Canada respectively. Henceforth, we will refer to the numerical model as ORCA12. The atmospheric conditions needed to force the model are provided by version 4.1 of the Drakkar forcing dataset (DFS4.1; Brodeau et al. 2010). The ORCA12 simulation starts from rest and is initialized from the *World Ocean Atlas 2005* climatological fields (Antonov et al. 2006; Locarnini et al. 2006) and covers the period from 1978 to 2007 and has been shown to simulate a realistic circulation in the North Atlantic (Marzocchi et al. 2015; Blaker et al. 2015; Duchez et al. 2014). Model output is available as 5-day averages. The observational data consist of geostrophic velocities computed from satellite altimetry and are produced by Ssalto/Duacs and distributed by Aviso, with support from CNES (<http://www.aviso.oceanobs.com/duacs>). The horizontal resolution of the geostrophic velocities is $1/4^\circ$ and the data are available as weekly values. Here we use data from 1993 to 2010. The observation based estimates of the Gulf Stream transport cover the period from 1982 to the present (Baringer and Larsen 2001; DiNezio et al. 2009; Meinen et al. 2010; Atkinson et al. 2010), but we use the period from 1993 to 2010. Gulf Stream transport data are available as daily mean values from <http://www.aoml.noaa.gov/phod/floridacurrent/>. For the purpose of this study the Gulf Stream data are interpolated on the weekly time resolution of the AVISO data. There are missing data for the Gulf Stream transport between 1998 and 2000 (funding gap) and September to October 2004 (damage during the passage of Hurricanes Frances and Jeanne; DiNezio et al. 2009). A linear interpolation is used to fill the gaps in the Florida Straits transport data.

The cable-based Florida Straits transport for the 1993–2010 period is 31 Sv with a standard deviation of 3 Sv (weekly averages). In the model the mean transport for the 1983 to 2007 period is also 31 Sv but the variability is weaker than in observations with a standard deviation of 2.1 Sv (5-day averages). For both the model and observational data we remove the long-term mean and unless stated otherwise we will use anomalies of velocity and transport in the remainder of the paper. Note that the accuracy of gridded satellite altimetry products near the coast has been questioned (e.g., Cipollini et al. 2017) which could be an issue for our study given that the Gulf Stream hugs the U.S. coast

between Florida and Cape Hatteras. The use of a numerical model (ORCA12) for which the same limitation does not apply mitigates against this. However, any model inevitably has deficiencies in its ability to simulate the real world due to, for example, limited resolution or approximations in the physics. When identifying precursors/successors of transport anomalies in the Florida Straits we will therefore concentrate on features which are seen in ORCA12 as well as in the satellite observations as these are the features that are most likely to be robust.

For both the model and observational data we use composite analysis to illustrate links between the transport through the Florida Straits and the large-scale surface velocity field. Composites ΔU^+ and ΔU^- are computed for anomalies of the absolute surface velocities ($U = \sqrt{u^2 + v^2}$, where u and v are the zonal and meridional velocity components) at the times t^+ and t^- when the transport anomalies through the Florida Straits are either positive or negative:

$$\Delta U^+(x, y) = \frac{1}{N^+} \sum_{i=1}^{N^+} \Delta U(x, y, t_i^+), \quad (1)$$

$$\Delta U^-(x, y) = \frac{1}{N^-} \sum_{i=1}^{N^-} \Delta U(x, y, t_i^-). \quad (2)$$

Parameters N^+ and N^- are the number of times when transport anomalies through the Florida Straits are positive or negative, and $\Delta U(x, y, t)$ are anomalies of the absolute surface velocity with respect to its long-term average \bar{U} :

$$\begin{aligned} \Delta U(x, y, t) &= U(x, y, t) - \bar{U}, \\ \bar{U} &= \frac{1}{t_s - t_e} \int_{t_s}^{t_e} U(x, y, t) dt. \end{aligned} \quad (3)$$

The start and end years t_s and t_e of the averaging period are 1993 and 2010 for the AVISO data and 1978 and 2007 for ORCA12. Unless stated otherwise no temporal filtering is applied to the model and satellite data. The composites ΔU^+ and ΔU^- are computed using 5-day and weekly averages for the model and the observations, respectively. To understand how anomalies develop and in particular to identify circulation anomalies that either precede or follow volume transport anomalies through the Florida Straits we also compute lagged composites. Throughout this paper a negative lag means that surface velocities lead the transport variability through the Florida Straits and for a positive lag it is the variability in the Florida Straits transports which leads the anomalies seen in the surface velocity field.

3. Results

In the following we illustrate the spatial coherence of surface velocities associated with transport anomalies through the Florida Straits and propose a simple continuity-based explanation linking the Loop Current in the Gulf of Mexico to the Gulf Stream transport through the Florida Straits.

a. Spatial coherence

The composites reveal striking coherence patterns (Fig. 1) that are similar for both the ocean model and the observations. At zero lag the strongest coherent signal stretches from southwest of Florida, to Cape Hatteras, and into the Gulf Stream Extension. Strong signals are also found in the Gulf of Mexico and to a lesser extent also in the Gulf Stream Extension. The most obvious difference between the model and the observation based composites is the extent of the coherence patterns. Whereas the signal is largely confined between the Gulf of Mexico and the Gulf Stream Extension in the observations, clear signals also occur farther south in the model. This is particularly the case along the coast of South America between the Equator and about 15°N. These differences will not be further discussed here and in the following we will concentrate on the features that are common to both the model and the observations from the Gulf of Mexico to Cape Hatteras.

In the Gulf of Mexico the sign of the composite signal changes when moving downstream along the Gulf Stream path. For positive composites (i.e., absolute surface velocity patterns coinciding with positive transport anomalies in the Florida Straits) the positive velocity anomalies found along Florida change to negative values when moving upstream into the Gulf of Mexico. The negative anomaly in the Gulf of Mexico is loop shaped. This is most clearly seen in the observations. In the model the spatial shape is similar but the eastern flank of the loop shaped anomaly is less pronounced than in the observations. Interesting features are also seen north of Cape Hatteras in both the model and the observations. The composites suggest that positive (negative) Gulf Stream transport anomalies coincide with a southward (northward) shift of the Gulf Stream Extension. In the model this can be seen most clearly just after the Gulf Stream detachment from the U.S. coast. Between longitudes of about 75° and 80°W the composite anomalies suggest a consistent meridional shift of 1°–2°. Moving farther eastward the composite anomalies become weaker and less coherent but they still suggest that the meridional shift extends well into the Gulf Stream Extension. In the observations the clear shift after Cape Hatteras is not seen, suggesting that it

may be a numerical feature of the model. However, farther east into the Gulf Stream Extension there is a meridional shift of about 1°–2°, which extends to about 60°W. For positive transport anomalies through the Straits of Florida we find predominantly positive velocity anomalies in the southern part of the Gulf Stream Extension, which are flanked by negative velocity anomalies to the north. This picture is reversed for negative transport anomalies through the Florida Straits: Here the southern part of the Gulf Stream Extension is characterized by predominantly negative velocity anomalies adjacent to positive velocity anomalies immediately to the north. The velocity anomaly patterns over the Gulf Stream Extension region are consistent with small meridional shifts of the Gulf Stream Extension. However, there are indications that the velocity anomalies indicative of a meridional shift in the Gulf Stream Extension are not significant. Changing the time period over which the composites are computed, the meridional shift can be present (e.g., during the first half of the model integration) or absent (second half of integration, not shown). In the following analysis we will therefore concentrate on the strongest composite anomaly signal seen between the Gulf of Mexico and Cape Hatteras both in the observations and in the model. In the model the Florida Straits transport also exhibits an underlying long-term (decadal) variability with a gradual increase of 2–3 Sv until 1990 which is followed by a decrease by a similar amount after that. No longer-term variability is evident in the cable observations of the Florida Straits transport.

To gain a dynamic picture of how the anomalies shown in Fig. 1 evolve in time, we look at lagged composites where Gulf Stream transport anomalies in the Florida Straits are related to the surface velocities either preceding or lagging them. In the model data we remove the long-term signal in the Florida Straits transport (red line in Fig. 1) and only retain subannual to interannual variability. We note that using the full variability does not change the basic links between the Loop Current and the Florida Straits transport we will describe below. However, removing the low-frequency variability leads to clearer pictures and better agreement with the observations. The temporal behavior of composite anomalies is most clearly seen in a movie (see supplementary material) but the main stages that have been identified are illustrated in Figs. 2 and 3). The lagged composites show that clear surface velocity anomalies are seen in the Gulf of Mexico about 6 weeks before the Florida Straits transport anomaly. These velocity anomalies are largest in the region where Loop Current eddies are known to develop. These positive velocity anomalies in the central Gulf of Mexico

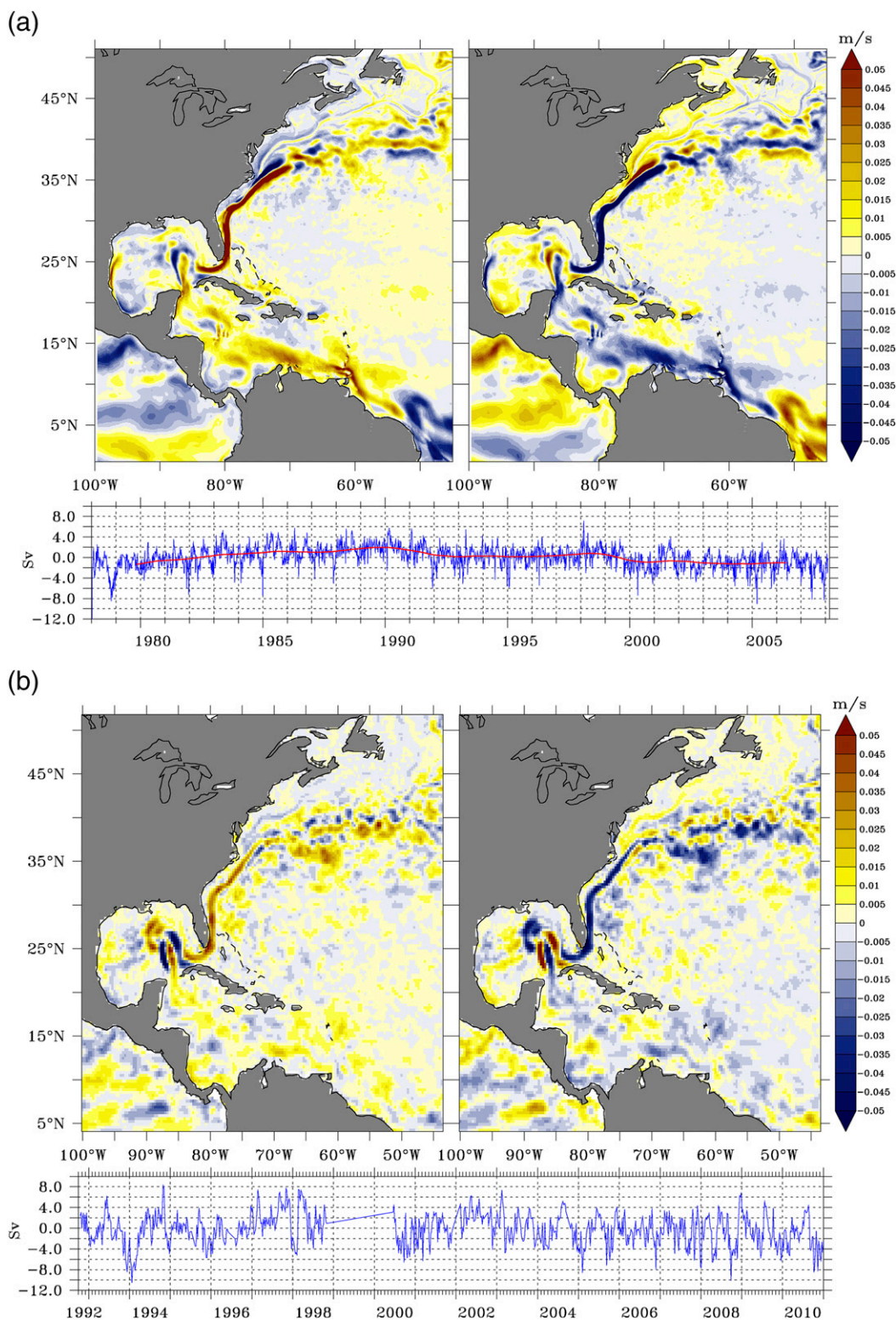


FIG. 1. (a) (top) Composites of absolute surface velocities for ORCA12. The positive and negative composites show the anomalous surface velocity pattern coinciding with (bottom) the positive and negative transport anomalies in the Florida Straits. The red lines in the bottom panel are the transport anomalies in the Florida Straits smoothed with a Parzen filter (window length of 1255 days). (b) As in (a), but for geostrophic surface velocities inferred from AVISO.

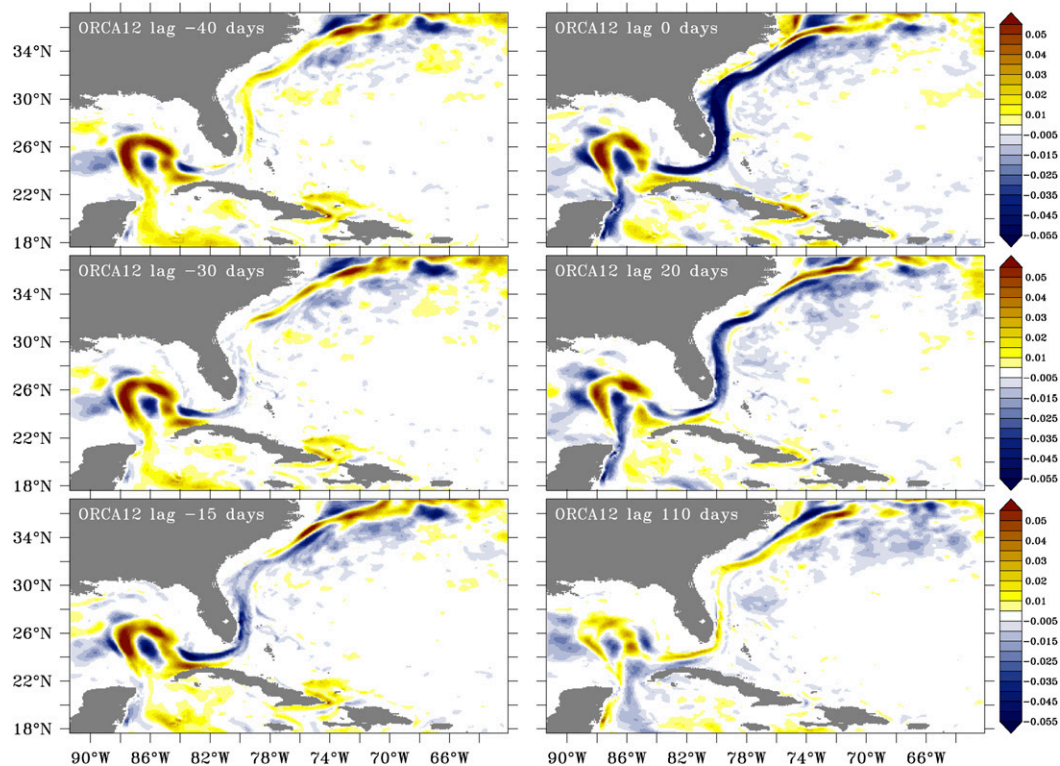


FIG. 2. Surface velocity anomalies (m s^{-1}) in ORCA12 coinciding with negative transport anomalies through the Florida Straits at lags of (top left to bottom left) -40 , -30 , and -15 days and (top right to bottom right) 0 , 20 , and 110 days. Positive and negative lags indicate that transport anomalies in the Florida Straits are leading and lagging, respectively, the surface velocity anomaly patterns in the Gulf of Mexico.

coincide with the development of a negative velocity anomaly to the southwest of the southern tip of Florida. Within about 2 weeks this anomaly then rapidly extends eastward and along the coast of Florida, through the Florida Straits, and toward Cape Hatteras. From its starting point to the southwest of Florida to Cape Hatteras it takes about 40 days for the anomaly downstream of the Gulf of Mexico to reach its maximum expression. Beyond Cape Hatteras the anomaly field becomes too noisy to be tracked farther into the Gulf Stream Extension. In the satellite data (between lags of 0 and 15 days) there is a decrease of the velocity anomaly along the southern part of Florida while the anomaly increases off Cape Hatteras and into the Gulf Stream Extension. In the model (between lags of 0 and 20 days) there is a decrease of the velocity anomalies everywhere from the Gulf of Mexico to Cape Hatteras. The velocity anomalies preceding and lagging the transport anomalies in the Florida Straits look like a “pulse” that rapidly propagates along the Gulf Streamflow. This pulse is somewhat reminiscent of the Natal pulses that occur in the Agulhas Current (Lutjeharms and Roberts 1988). However, as we will show next the mechanism is different here. Whereas Natal pulses are solitary meanders

that result from anticyclonic eddies propagating along and interacting with the Agulhas current (Lutjeharms and Roberts 1988; de Ruijter et al. 1999; van Leeuwen et al. 2000; Tsugawa and Hasumi 2010) the pulses described in this study are velocity anomalies (without any obvious meanders) which result from changes in the length of the Loop Current and the shedding of eddies.

b. Loop Current length and downstream transport

As mentioned earlier the composite anomalies that precede the appearance of the anomaly southwest of Florida are loop shaped (Figs. 2 and 3). A striking feature is that the loop shaped anomaly in the Gulf of Mexico and the anomaly that propagates along the U.S. coast are of opposite signs. To explain this feature we introduce a conceptual model (Fig. 4). For simplicity we consider the Gulf Stream as a continuous river whose average path is indicated as a blue ribbon. During the formation of a Loop Current eddy (Fig. 4a, red ribbon) the length of the Loop Current path increases: rather than remaining confined to the eastern part of the Gulf of Mexico the Loop Current path extends well into the interior of the Gulf. As the Loop Current increases in length the water flowing into the Gulf of Mexico goes

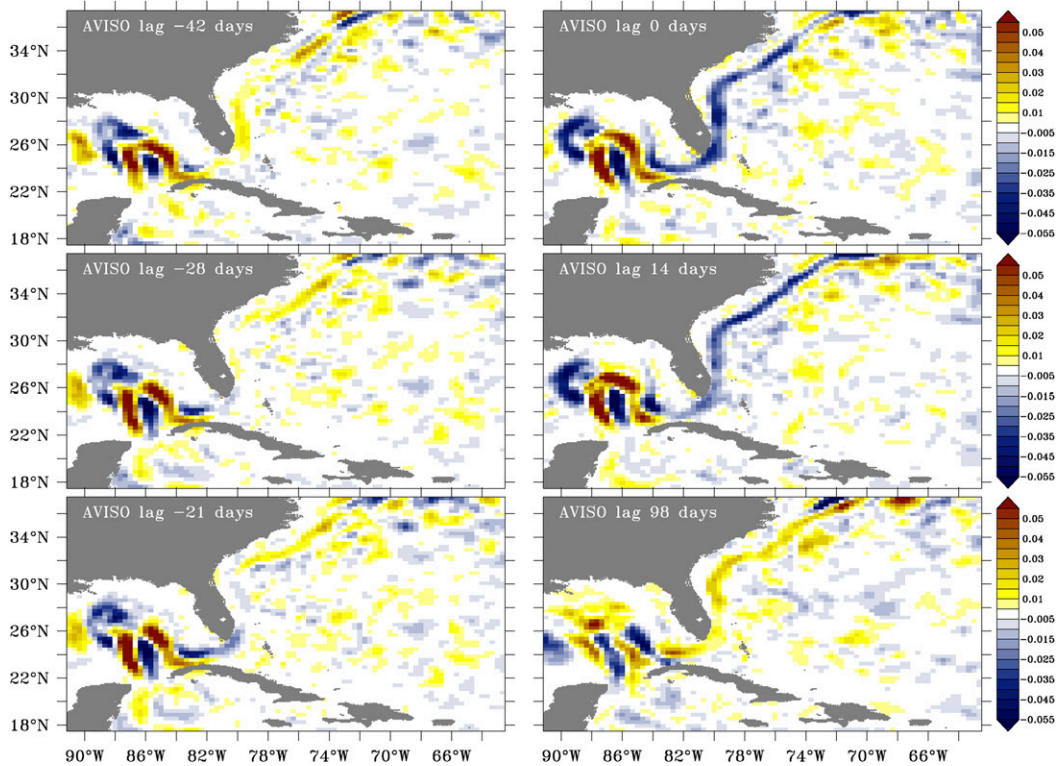


FIG. 3. Geostrophic surface velocity anomalies (m s^{-1}) from AVISO coinciding with negative transport anomalies through the Florida Straits at lags of (top left to bottom left) -42 , -28 , and -21 days and (top right to bottom right) 0 , 14 , and 98 days.

into lengthening the path. As a consequence the Gulf Stream transport at the outflow of the Gulf of Mexico will be reduced as the Loop Current expands. This reduction in transport will first be visible at the Gulf Stream outflow from where (consistent with Figs. 2 and 3) it will then propagate along the coast of Florida, through the Florida Straits and then farther northward toward Cape Hatteras. The opposite happens when a Loop Current eddy has been shed: the Loop Current path shortens (Fig. 4b, blue ribbon) and the Gulf Stream transport at the outflow of the Gulf of Mexico increases, triggering a positive velocity and transport anomaly which propagates toward Cape Hatteras. Note that the shedding of a Loop Current eddy is not necessary for there to be an imprint on the transport through the Florida Straits. The Loop Current can also contract without an eddy being formed. Using this simple continuity argument the relationship between the flow through the Florida Straits and the Loop Current length can be described as

$$T_{\text{FS}} = T_{\text{Yu}} - A \frac{\partial L}{\partial t}, \quad (4)$$

where T_{Yu} and T_{FS} are the flow into (Yucatan Channel) and out of the Gulf of Mexico through the Florida

Straits; A is the Gulf Stream cross section and L is the Gulf Stream length between Yucatan and the Florida Straits. For simplicity we assume T_{Yu} to be constant at 30 Sv and for A we assume the Gulf Stream width to be 50 km and its depth to be 500 m . Note that Eq. (4) assumes the flow out of the Gulf of Mexico to be a perfect indicator for T_{FS} , and previous work has shown that this is not necessarily the case (Hamilton et al. 2005). However, as we will show later the variability of the flow out of the Gulf of Mexico can explain more than 60% of the variance in T_{FS} in our model.

To get an estimate of changes in T_{FS} linked to the Loop Current from Eq. (4) we assume the length of the Loop Current to vary by 500 km between the shortest and longest paths. For the purpose of illustration we assume a temporally sinusoidal lengthening and shortening of the Loop Current length, that is, $L(t) = L_0 \cos(2\pi\omega t)$ and $\omega = 1/\tau$ is varied for periods τ between 1 year and 2 months and $L_0 = 250 \text{ km}$. The periods are chosen to cover the typical time scales for Loop Current eddy formation and shedding (one, occasionally two, Loop Current eddies are shed per year). Inserted into Eq. (4) this leads to

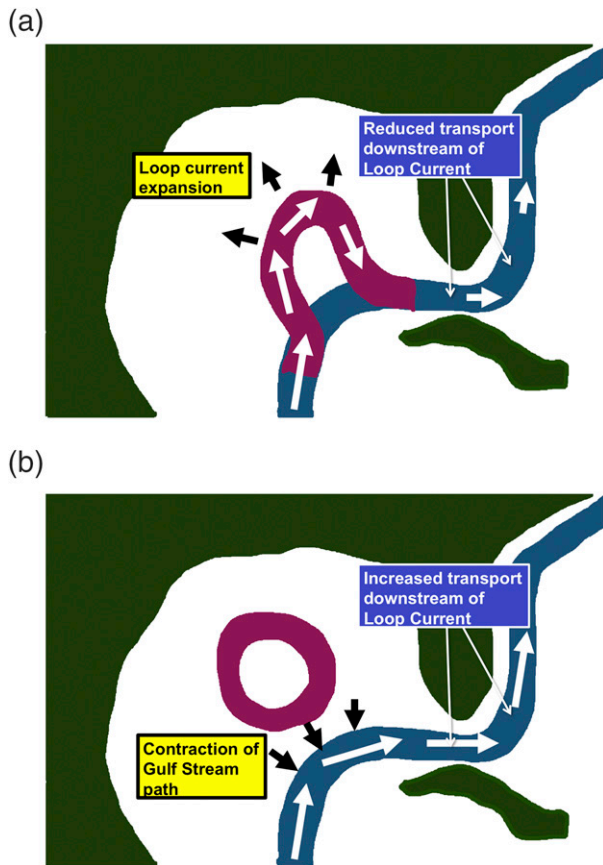


FIG. 4. Schematic illustrating link between Loop Current eddy formation and Gulf Stream transport.

$$T_{\text{FS}} = T_{\text{Yu}} + AL_0\pi\omega \sin(2\pi\omega t), \quad (5)$$

where $AL_0\pi\omega$ is the amplitude of the transport variability in T_{FS} . According to Eq. (5) this expansion and contraction of the Loop Current length leads to transport anomalies of several Sverdrups downstream of the idealized Loop Current. The higher the frequency ω are (generally, the faster the rate of length change), the larger the changes in Florida Straits transport T_{FS} become. For the idealized values given above we find amplitudes of 1.2 Sv ($\tau = 1$ year) to 7.2 Sv ($\tau = 2$ months) for T_{FS} . Note that expansion/contraction of the Loop Current length and transport anomalies are not in phase. Transport anomalies reach maximum values when the rate of change in pathlength reaches its maximum. In the simple example chosen here the time series of transport anomalies is shifted by 90° with respect to the pathlength. Obviously, the view presented above is highly idealized: the Gulf Stream is not just an “oceanic river” with given width and depth that occasionally sheds eddies. The Gulf Stream is a variable current with spatiotemporal changes in both its width and depth.

Nevertheless, it is between the inflow in Yucatan to Cape Hatteras that the Gulf Stream is at its most coherent (Fig. 1) and it is only when the Loop Current becomes unstable while shedding Loop Current eddies that the flow cannot be identified as a coherent flow band. This provides the motivation and some justification for the assumptions we make here [Fig. 4, Eqs. (4) and (5)] and the simple considerations above suggest that the variability in the Loop Current pathlength could be an important contributor to the variability of the transport through the Florida Straits. Note that the mass imbalance implied from Eq. (4) only applies to the “river” through the Gulf of Mexico. An accumulation or deficit of volume transport into the Gulf of Mexico would result in significant sea level change (about 5 cm day^{-1} for an imbalance of 1 Sv). Such changes are neither observed in the real ocean nor simulated in our model so any imbalance occurring according to Eq. (4) will be largely compensated when considering not just the “river” but the transports through the full sections between Yucatan and Cuba and between Florida and Cuba. We will get back to this point later in this section.

In a next step we define a metric for the variability in the Gulf Stream length to establish whether we can see an imprint of Loop Current length variability on the transport through the Florida Straits in the real North Atlantic and in ORCA12. We developed an algorithm that tracks the Gulf Stream path by following the highest absolute surface velocity. With this “pathfinder” algorithm we can determine the Gulf Stream path and length for each time step (5-day averages for the model, weekly values for AVISO). The length of the Gulf Stream path is computed between the northeastern edge of the Yucatan Peninsula and the Straits of Florida. The northeastern edge of Yucatan is where the Yucatan Current enters the Gulf of Mexico and both in the model and observations the strongest flow hugs the coast of Yucatan for most of the time. The starting point $(x, y)_0$ of the path is where we find the highest velocity between Yucatan and Cuba when following the latitude of 21.5°N eastward:

$$(x, y)_0 = \text{loc} \left\{ \max \left[\sqrt{u^2(x, y_{21.5^\circ\text{N}}) + v^2(x, y_{21.5^\circ\text{N}})} \right] \right\}. \quad (6)$$

Generally, the location $(x, y)_0$ is found to be right at the coast of the Yucatan. Starting from $(x, y)_0$ the pathfinder algorithm follows the Gulf Stream path into the Gulf of Mexico and out through the Florida Straits up to Cape Hatteras by scanning the eight neighboring grid points.

The decision from one step $(x, y)_n$ to the next step $(x, y)_{n+1}$ along the Gulf Stream path is based on both the amplitude of the current speed in the neighboring cells

as well as on the heading the flow has at point $(x, y)_n$. If i, j denote the grid coordinates of the path location $(x, y)_n$ the next location $(x, y)_{n+1}$ is found according to

$$(x, y)_{n+1} = \text{loc} \left[\max(w_{i,j+1} U_{i,j+1}, w_{i+1,j+1} U_{i+1,j+1}, w_{i+1,j} U_{i+1,j}, w_{i+1,j-1} U_{i+1,j-1}, \right. \quad (7)$$

$$\left. w_{i,j-1} U_{i,j-1}, w_{i-1,j-1} U_{i-1,j-1}, w_{i-1,j} U_{i-1,j}, w_{i-1,j+1} U_{i-1,j+1} \right), \quad (8)$$

where the values of the weights w depend on the heading of the flow at the location $(x, y)_n$. The weighting w is highest for the grid cells in the direction into which the velocity vector (u_n, v_n) is pointing. For a velocity vector consisting of positive northward and eastward components v and u , the weights w are set to $w = 20 + \sin(\alpha)$, $w = 20 + \tan(\alpha)$, and $w = 20 + \cos(\alpha)$ for points $(i, j + 1)$, $(i + 1, j + 1)$, and $(i + 1, j)$, respectively, where α is the angle between the velocity vector (u, v) and an eastward-pointing vector. The weight is set to $w = 6$ for the neighboring points $(i - 1, j)$ and $(i + 1, j - 1)$ and $w = 1$ for the remaining neighbors. Using much higher weights for the neighbors in the direction in which the flow is heading markedly reduces instances of the computed Gulf Stream path ending in a closed loop and the empirical values of 1, 6, and 20 were found to provide a faithful tracking of the maximum velocities along the Gulf Stream. Note that there can still be times when the Gulf Stream path ends up “trapped” in the Gulf of Mexico so that it never reaches the Florida Straits. This typically occurs when the Loop Current is in the process of shedding an eddy as during such periods the Gulf Stream flow between Yucatan and the Florida Straits no longer consists of a coherent stream. To avoid the path algorithm returning an undefined path the Gulf Stream path is set to the trajectory found for the last time step for which a valid path was returned, that is, a path that enters the Gulf of Mexico off northeastern Yucatan and exits it through the Florida Straits.

The densities of Gulf Stream pathways inferred from satellite data and simulated by ORCA12 are shown in Fig. 5. Very similar probabilities are found for the simulated and observed Gulf Stream paths. When considering all paths, the highest probability is found for paths that extend well into the Gulf of Mexico. For both in the model and observations the highest probabilities indicate a loop that is oriented northwestward and is bound to the northeast by the West Florida Shelf and to the southeast by the Campeche Bank off the Yucatan

Peninsula. The average length obtained when following the highest probabilities is about 1200 km. However, even though less likely, much shorter and longer paths also occur. The shortest ones (about 600 km in length) have hardly any incursion into the Gulf of Mexico and closely follow the northern coast of Cuba before entering the Florida Straits. The longest paths extend well into the Gulf of Mexico with lengths of 1500 km or more. Apart from a few exceptions all the Loop Current paths obtained in ORCA12 and in the observations are confined to the Abyssal Plain of the Gulf of Mexico. The highest density of paths occur to the northeast of Yucatan and along the east coast of Florida. Both for the model and the observations every single path that can successfully be computed goes through the Florida Straits. Between 24° and 28°N in the Gulf of Mexico there is a slightly higher probability of long paths extending westward beyond 90°W in the observations compared to ORCA12 suggesting that the model does not quite accurately represent the dynamics of the Loop Current. Another subtle difference between model and observations can be found along the coast of Florida north of about 30°N: whereas all the paths computed in the model basically follow the same trajectory with only a gradual dispersion of paths when moving northward, there are some paths peeling off into the basin interior in the observations. This suggests that the actual Gulf Stream along the U.S. East Coast up to Cape Hatteras may be less stable than its modeled counterpart. Despite such differences the Gulf Stream path is well defined for most time steps for the observational and for the model data.

To test whether the relationship between Florida Straits transport and Loop Current length proposed in Eq. (5) holds we select paths coinciding with either strong or weak transports. The threshold for selection is chosen as 1.5 times the standard deviation of the Florida Straits transport (Fig. 5, middle and bottom panels). This threshold ensures that enough paths are retained for the probabilities while focusing on transports that

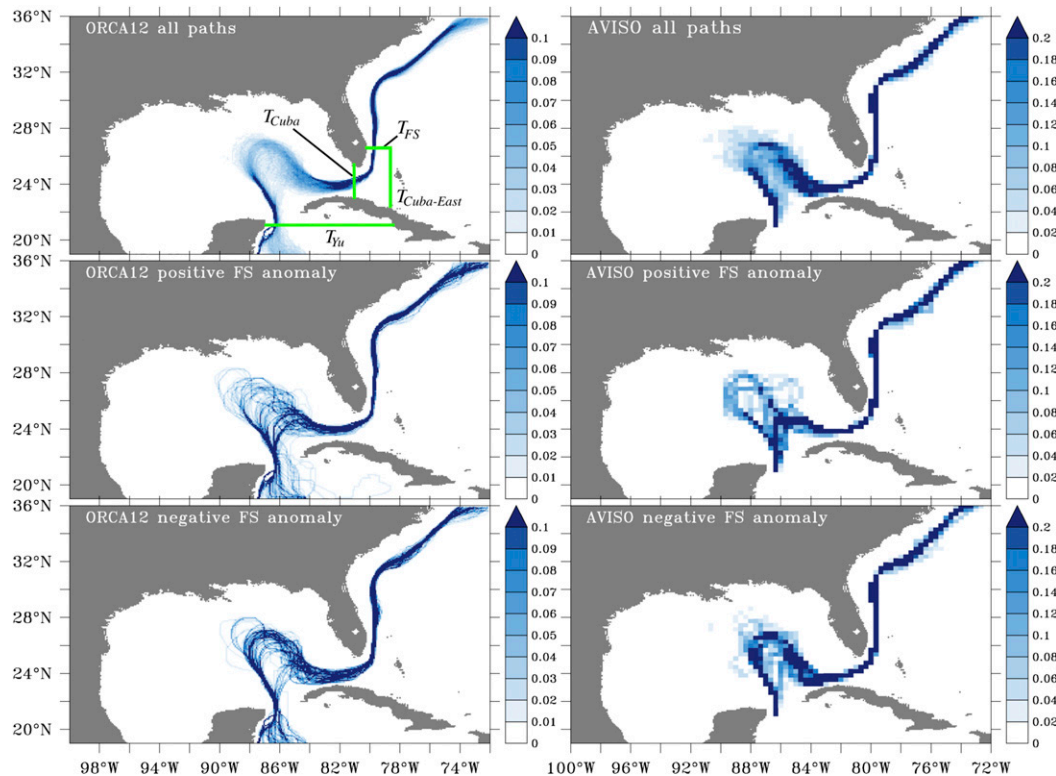


FIG. 5. Gulf Stream path distributions for (left) ORCA12 and (right) AVISO. Gulf Stream paths are computed for each weekly field between 1993 and 2010 for ORCA12 and for each 5-day average between 1983 and 2010 in AVISO. The distributions show (top) all paths, (middle) paths coinciding with Florida Straits transports anomalies >1.5 standard deviations, and (bottom) paths coinciding with Florida Straits transports <-1.5 standard deviations. (top left) The green lines indicate the sections across which the transports are computed and shown in Fig. 6.

are clearly stronger/weaker than the mean. We find a remarkable agreement between the model and the observations. Compared to the probabilities obtained using all paths there is a higher probability of short paths when only considering times when the transport is strong. The opposite holds true for weak transports and the highest probabilities are found for paths that extend well into the Gulf of Mexico. The link between pathlength and transports is weaker for positive than for negative transport anomalies. Even though the highest probabilities are found for short paths when transports are strong it is also clear that a strong Florida Straits transport can also coincide with intermediate and long paths. In comparison we find only few short paths coinciding with weak transports through the Florida Straits. There is also a tendency for a more binary behavior in this case with paths either being long or short with hardly any paths of intermediate length. Despite a range of pathlengths being found to coincide with above or below average transport through the Florida Straits the results shown in Fig. 5 support the view that the length of Loop Current can

be indicative of the transport strength through the Florida Straits.

The close agreement between observations and the model motivates the use of the latter to further investigate how strongly Loop Current activity affects the transport through the Florida Straits. The availability of the full 3D velocity fields in the model means that transports in and out of the Gulf of Mexico can be studied in more detail (Fig. 6). The conceptual model introduced in Eq. (5) assumes that between Yucatan and the Straits of Florida the Loop Current can be regarded as a “river.” This river is confined to the surface part of the ocean and the northward transport into the Gulf of Mexico occurs in the top 700 m. The 0–700-m-depth range covers most of the cross section between Cuba and Florida and hence most of the net transport out of the Gulf of Mexico toward the Florida Straits. Relating transports between Yucatan and Cuba T_{Yu} as well as between Cuba and Florida T_{Cuba} to the Florida Straits transport T_{FS} shows a markedly higher correlation between T_{Cuba} and T_{FS} ($r = 0.79$, 62% explained variance) than between T_{Yu} and T_{FS} ($r = 0.59$, 35%

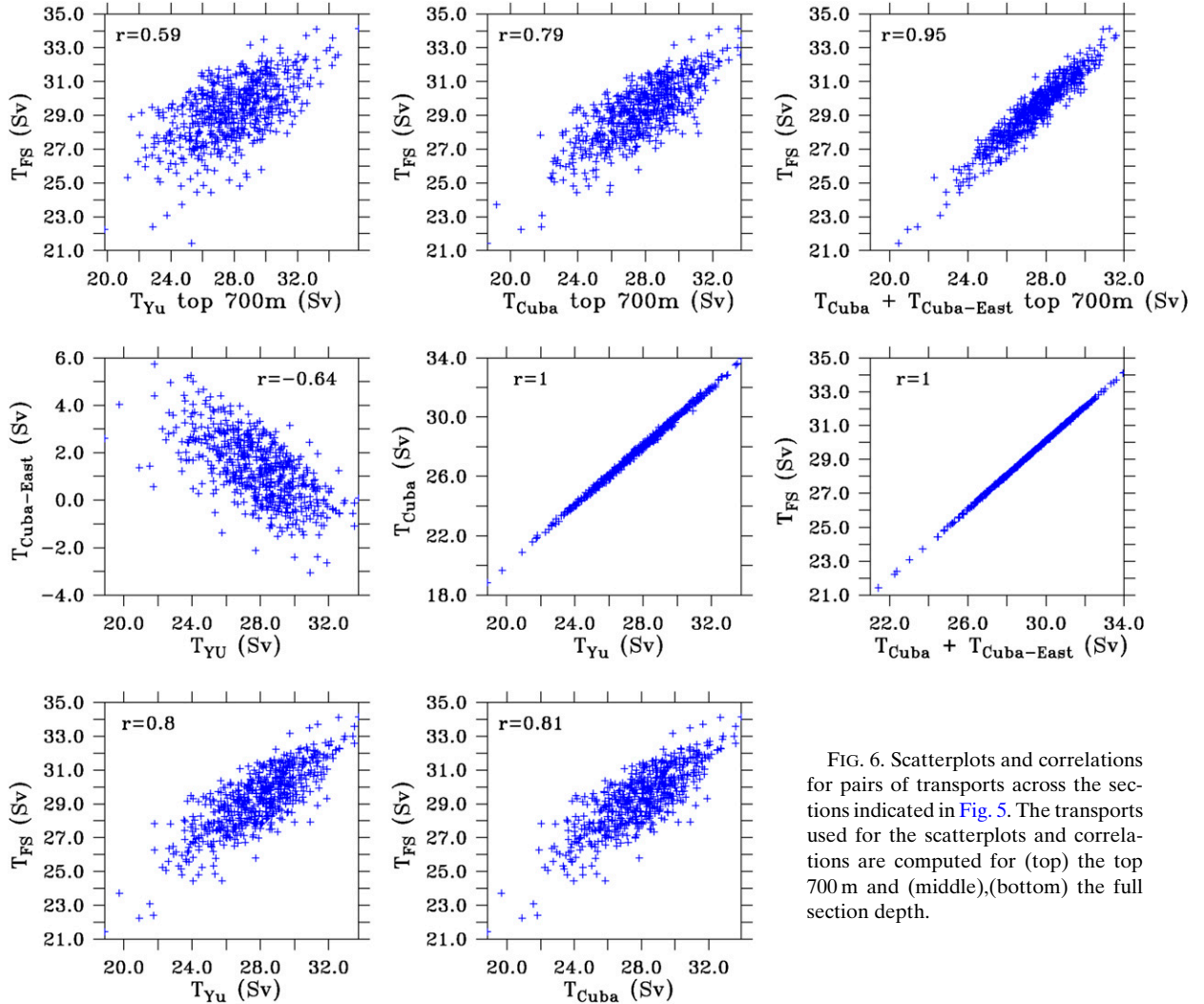


FIG. 6. Scatterplots and correlations for pairs of transports across the sections indicated in Fig. 5. The transports used for the scatterplots and correlations are computed for (top) the top 700 m and (middle),(bottom) the full section depth.

explained variance). Taking into account the transport in the top 700 m between the Bahamas and Cuba $T_{\text{Cuba-East}}$ allows more than 90% of the variance of the Florida Straits transport to be recovered [correlation $r(T_{\text{Cuba}} + T_{\text{Cuba-East}}, T_{\text{FS}}) = 0.95$]. Looking at full depth transports for the same sections we get $r(T_{\text{Yu}}, T_{\text{Cuba}}) = 1$. Consistent with that the correlations $r(T_{\text{FS}}, T_{\text{Yu}}) = 0.8$ and $r(T_{\text{FS}}, T_{\text{Cuba}}) = 0.81$ are almost identical. This means that (in the model at least) any mass storage term in the Gulf of Mexico linked to changes in the Loop Current length is negligible and that as we mentioned earlier there must be a compensation for the imbalance between the in- and outflow in the top 700 m. This compensation is captured when integrating transports over the full depths of the sections between Yucatan and Cuba B and between Cuba and Florida C . Considering full depth transports and assuming spatially uniform compensations through the channels the relation

between the river transport into T_{Yu} and out of T_{Cuba} the Gulf of Mexico can be written as

$$T_{\text{Yu}} + \frac{\beta A}{B} \frac{\partial L}{\partial t} \int_{x_1}^{x_2} dx \int_{-H_{\text{Yu}}}^0 dz + \frac{\gamma A}{C} \frac{\partial L}{\partial t} \int_{y_1}^{y_2} dy \int_{-H_{\text{Cuba}}}^0 dz - A \frac{\partial L}{\partial t} = T_{\text{Cuba}}, \quad (9)$$

where $\beta + \gamma = 1$. The integration limits x_1, x_2 and y_1, y_2 are the zonal and meridional end points of the Yucatan-Cuba (B) and Cuba-Florida (C) sections; H_{Yu} and H_{Cuba} are the maximum depths of the respective sections. The second to fourth terms on the left-hand side of Eq. (9) cancel each other out when integrating over the full cross sections. However, when considering the transports through the “river” cross section A these terms no longer compensate and Eq. (9) can be written as

$$T_{Yu} + A^2 \frac{\partial L}{\partial t} \left(\frac{\beta}{B} + \frac{\gamma}{C} \right) - A \frac{\partial L}{\partial t} = T_{Cuba}, \quad (10)$$

In contrast to Eq. (4), Eq. (10) contains a compensation term (second left-hand term) for the mass imbalance linked to the temporally changing length L . Only a fraction (A/B and A/C , respectively) of the compensations across sections B and C directly projects onto the river flow in and out of the Gulf of Mexico. Given the larger and deeper cross-sectional area B between Yucatan and Cuba than between Cuba and Florida C a larger fraction of the compensation is likely to flow through the former section (i.e., $\beta > \gamma$). This is supported by the lower correlation we find between T_{Yu} and T_{FS} than between T_{Cuba} and T_{FS} (Fig. 6). A compensation occurring mainly between Cuba and Florida is therefore unlikely. In the extreme case of all compensation occurring between Cuba and Florida (i.e., $\beta = 0$, $\gamma = 1$) the correlations $r(T_{Cuba}, T_{FS})$ and $r(T_{Yu}, T_{FS})$ would have to be almost identical in the top 700 m as the top 700 m encompass most of the section between Cuba and Florida. However, the correlations presented in Fig. 6 show that this is not the case. Identical correlations are only found when full depth transports are used across both sections.

c. Timing of Loop Current and Florida Straits transport

Having established that the variability in the Loop Current length is linked to the transport downstream of the Gulf of Mexico, a natural question to ask is whether one can use the Loop Current length to predict transport anomalies through the Straits of Florida. The simple model in Eqs. (4) and (5) suggests that there should be a phase shift of $\pi/2$ between both time series. However, this rests on the assumptions that as the Loop Current expands or contracts its depth and width does not change, and that the length of the Loop Current varies periodically. This obviously does not have to be true meaning that even if Loop Current variations project onto the Florida Straits transport the phase relation between the Loop Current pathlength and the Florida Straits transport could change temporally. As a first step it is therefore useful to compare the spectra found in the temporal variability of the Florida Straits transport and of the Loop Current pathlength (Fig. 7). A wavelet analysis shows that for both the variability of the Florida Straits transports and of the Loop Current length most power is found for periods of 6 months or longer. This is the case in the model as well as in

the observations. Cross-coherence is also strongest for periods of about 2–4 months or longer. Phases of significant cross-coherence occur for both the model and the observations. These phases are mainly confined to periods between 2 and about 6 years. There is indication of coherence on longer time scales but given the length of the time series confidence is low. The cross-coherence also shows that there is no consistent phase relationship between the Gulf Stream path variability and the Florida Straits transport. However, most phases of significant coherence have in common that the phase difference between the signals varies from about π (i.e., signal in antiphase phase, arrows pointing to the left) and about $\pi \pm \pi/2$ (arrows still broadly pointing to left but with an upward or a downward component). This is broadly consistent with high (low) transports through the Florida Straits occurring during phases of short (long) Loop Current length.

The cross-coherence can further be illustrated looking at the actual time series for Florida Straits transport and Loop Current length anomalies (Fig. 8). The time series of the Gulf Stream pathlength and of the Florida Straits transport show that most peaks and troughs in transport have a counterpart in the Gulf Stream length (Fig. 8). However, as shown in the wavelet cross-coherence analysis the phase shift between transports and pathlength for the simulated and observed Gulf Stream varies in time. There are times when the time series are mainly out of phase (e.g., from 1983 to about 1990 in the model) or in phase (e.g., from 2004 to 2006 in the observations) and there are also instances when the phase shift seems close to the $\pi/2$ suggested in our simple conceptual model (e.g., 1997–99 in observations or 2003–04 in the model). Whereas the number of peaks and troughs in transport and pathlength suggests a link between Loop Current expansion and contraction and volume transport through the Florida Straits, it is also clear that such a relationship can only partly be explained by the simple model based on continuity considerations, as suggested in Eqs. (4) and (5).

4. Discussion and conclusions

Our results confirm earlier findings by Lin et al. (2010) and Mildner et al. (2013), who show that the evolution of the Loop Current can impact the Gulf Stream transport through the Florida Straits. In these earlier studies the authors suggest that either interactions between the Loop Current and topography (Lin et al. 2010) or the presence of a ring north of Yucatan which reduces the flow into the Gulf of Mexico

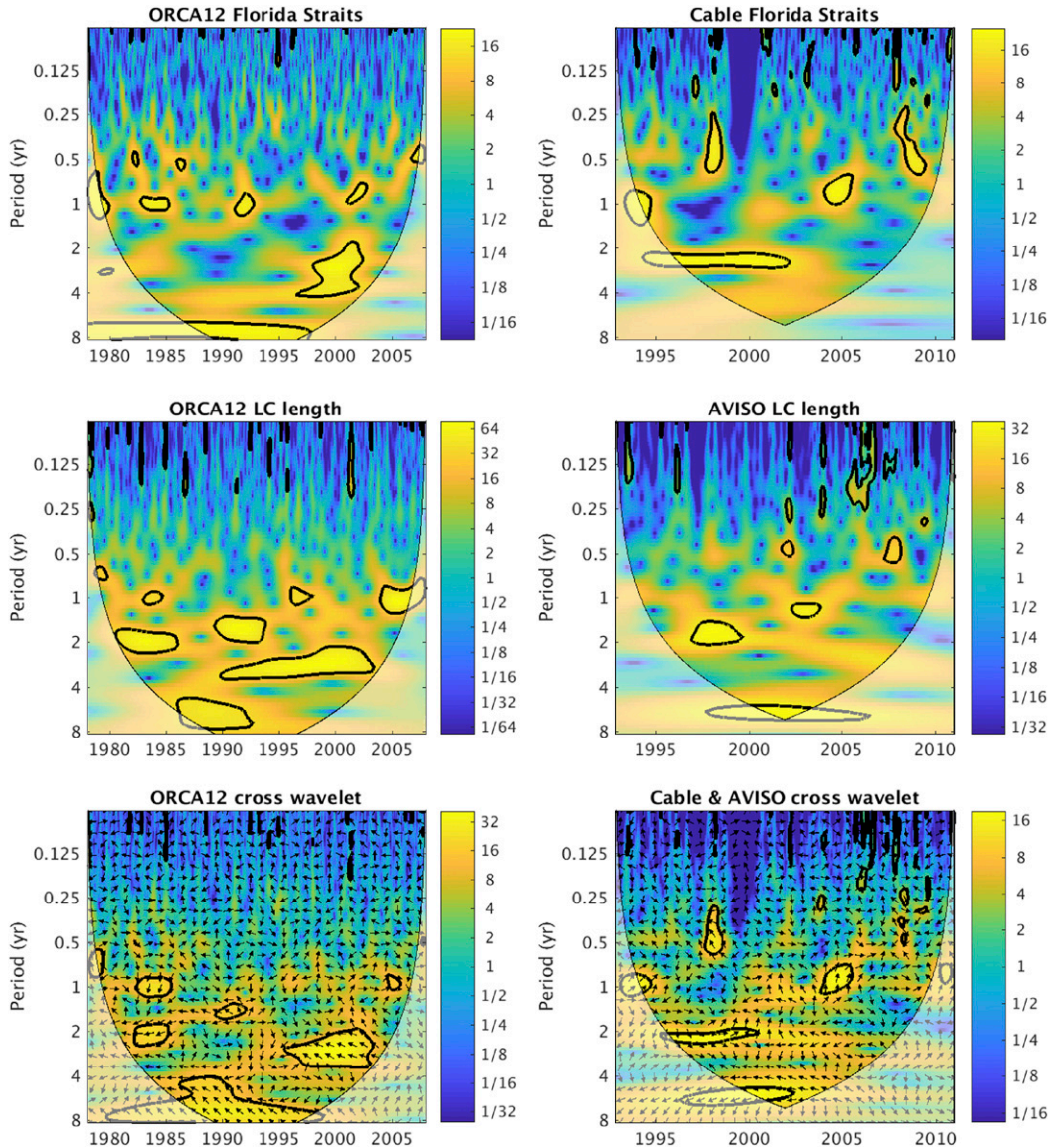


FIG. 7. Wavelet analysis (top) for Florida Straits transport and (bottom) for time series of Loop Current length. Results are shown for (left) ORCA12 and (right) AVISO. (bottom) Wavelet cross-coherence between Florida Straits transport and variability of Loop Current length. The units for the period are years, and bold contours indicate when the time series for Florida Straits transport or the Loop Current length have statistically significant periodicities and when the coherence between both time series is statistically significant ($p < 0.05$). Shading indicates either the wavelet power density or the coherence (both in arbitrary units). Arrows for the coherences indicate the phase between the time series. Arrows pointing to the right (left) indicate signals are in phase (out of phase).

(Mildner et al. 2013) can lead to reductions in the volume transport through the Florida Straits. Here, we have presented an additional view on how the Loop Current is likely to affect the flow downstream of the Gulf of Mexico. Using a simple continuity argument a lengthening (shortening) of the length of the Loop Current should lead to a decrease (an increase) in the Gulf Stream transport downstream of the Loop Current.

Our results suggest that the lengthening (shortening) of the Loop Current leads to pulses in the Gulf Stream transport that rapidly—within a few weeks—propagate from southern Florida to Cape Hatteras and that are triggered by expansion (contraction) of the Loop Current. These pulses can be identified both in a high-resolution ocean model as well as in observations of the real ocean (Figs. 2 and 3 and supplementary material).

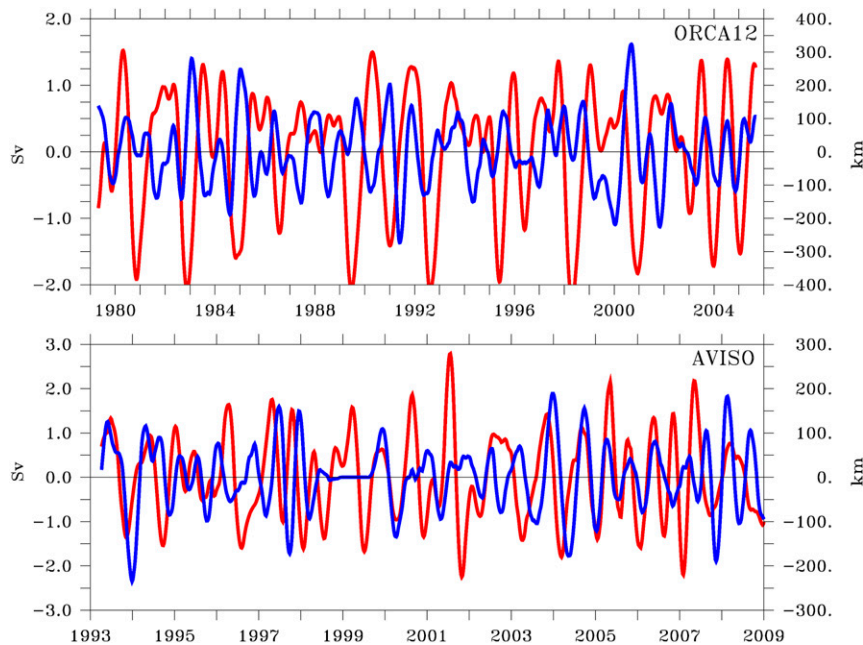


FIG. 8. Time series for anomalies of Gulf Stream transport (blue; left axis; Sv) and Loop Current length (red; right axis; km) for (top) ORCA12 and (bottom) AVISO. Time series for transports and pathlengths have been high- and low-pass filtered to retain only seasonal to interannual time scales where the strongest coherence is seen in Fig. 7. The correlations between the Loop Current length and Florida Straits transport anomalies are -0.24 (ORCA12) and 0.13 (AVISO).

The fact that we see these pulses both in the model and observations provides some confidence that we are looking at a robust signal and not just at an artifact of the model, or at a feature linked to limitations of satellite observations in coastal regions. Therefore, our results provide a strong indication that the Loop Current is likely to be a major contributor to the Gulf Stream variability farther downstream along the coast of Florida and up to Cape Hatteras, in particular to its chaotic variability. Indeed, whereas the Loop Current is known to affect air–sea interactions (e.g., Putrasahan et al. 2017), the actual timing of changes in the Loop Current is largely unpredictable from surface forcing (Oey et al. 2003; Oey et al. 2005) and results from baroclinic instability of the Loop Current (e.g., Donohue et al. 2016b), vorticity pulses from the Caribbean (Sheinbaum et al. 2016), and/or coastally trapped waves originated within the Gulf of Mexico (Jouanno et al. 2016). As a consequence, movements of the Loop Current and the shedding of Loop Current eddies are largely chaotic (Donohue et al. 2016a).

Our study suggests that the expansion and contraction of the Loop Current can account for variations of several Sverdrups in the Gulf Stream transport through the Florida Straits on subannual time scales

[Eq. (5), Fig. 8]. However, comparing time series of the Loop Current length and of the downstream volume transport also shows that the link between the two quantities is not as straightforward as in the simple model described by Eq. (4). For both the modeled and observed time series the lead–lag relation between the variability in Loop Current length and Florida Straits transport varies during the periods considered which means that the correlation between the two quantities is not high ($r = -0.24$ for ORCA12 and $r = 0.13$ for AVISO). It is also worth noting that there is also no clear link between the amplitudes of the changes in pathlength and the transport variability. Nevertheless, even if not consistently aligned with the same lag, almost all peaks and troughs in the Gulf Stream transport through the Florida Straits have a counterpart in the variability of the Loop Current length. Together with the composite analysis showing the coherence and pulses of the Gulf Stream this supports the view that the waxing and waning of the Loop Current projects onto the Gulf Stream farther downstream through the Florida Straits and up to Cape Hatteras. At this point it is also worth reminding ourselves that particularly in the model, and to a lesser extent also in the observations there are downstream signals in the Caribbean Sea and along South America (Fig. 1). These signals

were not the focus of the present study but they may be indicative of precursors for the Loop Current variability.

The Gulf Stream is part of the wind-driven circulation. The action of the winds (via the wind stress) together with Earth's rotation explain the strength and structure of the Gulf Stream. Being highly variable on all time scales winds are also a major source of variability for the Gulf Stream on subannual and longer time scales (Anderson and Corry 1985; DiNezio et al. 2009; Atkinson et al. 2010; Sanchez-Franks et al. 2016). However, these studies also show that variability in the wind stress is not sufficient to fully explain the variability in the western boundary current system comprising the Gulf Stream, the Yucatan Current, and the Loop Current, and a large fraction of the transport variability through the Florida Straits has a different origin. In particular, to understand transport variability in the Gulf Stream through the Florida Straits the intrinsic/chaotic variability of the ocean has to be taken into account as well. Our study supports the view that this chaotic ocean variability is likely to account for a large, possibly even the largest fraction of the Gulf Stream variability on sub to interannual time scales. This chaotic variability in the ocean is linked to eddy and internal wave activity. In the case of the Gulf Stream eddies and waves can impact the transport as they approach the coast and start to interact with the western boundary current system (e.g., Clément et al. 2016; Clément et al. 2014; Frajka-Williams et al. 2013, Kanzow et al. 2009; Zhai et al. 2010; Sinha et al. 2013, Hirschi et al. 2007). Alternatively western boundary currents can themselves produce eddies. In this case eddy formation starts as meanders in a coherent current which grow until they eventually break. This is seen, for example, in the Kuroshio and Gulf Stream Extensions or as in this study in the Gulf of Mexico. It is these eddies that start as meanders that are at the heart of the ideas developed in Lin et al. (2010) and Mildner et al. (2013) as well as in the present study. Impacts of eddies on the temporal variability of the volume transport through the Florida Straits are likely to have different origins. Such impacts can be linked to a local interaction of eddies with the current as they approach Bahamas from the basin interior (Frajka-Williams et al. 2013; Clément et al. 2014; Clément et al. 2016). However, it is also conceivable that eddies (or generally westward propagating features) reaching the coast farther north could also affect the transport through the Florida Straits. In this case perturbations could be mediated toward the Florida Straits as boundary trapped waves (e.g., Zhai et al. 2010; Sinha et al. 2013). To our knowledge

such a situation has not yet been observed for the transport through the Florida Straits. However, the concept of westward perturbations triggering equatorward, boundary trapped waves is well established in theory and in numerical modeling studies (e.g., Liu et al. 1999; van Sebille and van Leeuwen 2007; Kanzow et al. 2009) and in observations boundary waves have been shown to affect transports in the boundary currents in the Gulf of Mexico (Dubranna et al. 2011).

When considering the Loop Current there are several ways in which the Gulf Stream transport downstream could be affected via this current:

- 1) Increases or decreases of the flow into the Gulf of Mexico without changes in the path/shape of the Loop Current. This could for example occur when eddies in the Caribbean Sea propagate westward toward northeastern Yucatan and attach to the Gulf Stream off Yucatan. In such cases anomalies through the Channel of Yucatan would essentially be passively advected along the Loop Current and into the Florida Straits. The transport through the Yucatan Channel can also vary in response to large-scale changes in the wind forcing over the region.
- 2) As the Loop Current expands, an anticyclonic eddy develops within the Loop Current which reduces the flow into the Gulf of Mexico by partly blocking the Yucatan Channel (Mildner et al. 2013). In this case the assumption is that the transport through the Florida Straits is modulated by the flow into the Gulf of Mexico and that changes in the Loop Current length do not affect the outflow through the Florida Straits.
- 3) In our study we propose a modulation of the Florida Straits transport as a response to the increase and decrease in length of the Loop Current based on a continuity argument along the current. In this case the transport through the Florida Straits can change even if the inflow via the "river-like" Yucatan Current into the Gulf of Mexico is temporally constant. Note that as indicated by Eq. (9) and Fig. 6 the full-depth transports across both sections *B* and *C* will be near identical at all times.

Whereas the mechanism proposed by Mildner et al. (2013) is consistent with a coherent transport/velocity anomaly between Yucatan and the Florida Straits (schematic in their Fig. 5), the mechanism we describe in the present study is consistent with the coherent transport/velocity anomalies which extend from southwest Florida to Cape Hatteras, something we find both in the model and the observations (Figs. 1–3). The mechanism as proposed by Mildner et al. (2013) can only be invoked to explain minima in the Florida Straits transport but does not provide an explanation

for transport maxima. In contrast, the mechanism proposed here can be used to explain the development of both positive and negative transport anomalies. Our continuity-based mechanism presented here implies that at times there is a net inflow into or out of the Gulf of Mexico but the model suggests that this imbalance is compensated across the full depths of the Yucatan–Cuba and Cuba–Florida sections. To understand how and where such a compensation occurs would require the volume of the Loop Current to be computed as function of time and then linked to the flow through the sections *A* and *B*. Both the calculation of the Loop Current volume as a function time and isolating the part of the cross-sectional flow associated with these volume changes are far from trivial, however. An in-depth analysis of the exact nature and structure of the compensation is therefore left for a future study.

Nevertheless, Eq. (10) suggests that a barotropic compensation would be consistent with the relationships between the flow in and out of the Gulf of Mexico shown in Fig. 6. However, it is likely that the compensation occurs as a consequence of processes of types 1, 2, and 3 working in concert. In particular the mechanisms proposed by Mildner et al. 2013 and Lin et al. (2010) and the mechanism proposed here are closely related. Part of the compensation required to, for example, compensate the net inflow as the Loop Current expands could follow the route south of Cuba suggested by Mildner et al. (2013) and the transport decrease through the Florida Straits could be the consequence of both a reduced inflow into the Gulf of Mexico as well as to a reduction due to the expanding pathlength of the Loop Current. It seems plausible that mechanisms 1, 2, and 3 would typically work in combination rather than in isolation. This also means that the downstream impact of the Loop Current is hard (if not impossible) to quantify as processes 2 and 3 are difficult to separate. What is clear though is that both 2 and 3 can potentially account for transport anomalies of several Sverdrups in the Florida Straits and therefore have the potential to explain a large fraction of the Florida Straits transport variability on subannual to perhaps interannual time scales. The chaotic nature of their timing means that they will also directly contribute to the intrinsic/chaotic variability in the Atlantic meridional overturning circulation as observed at 26.5°N (Smeed et al. 2014). What our study has also shown is that transport anomalies linked to the variability of the Loop Current are not confined to the Straits of Florida but extend all the way to Cape Hatteras where they may affect the Gulf Stream trajectory after its separation from North

America and the stability of the flow in the Gulf Stream Extension. This therefore suggests that there may be a direct link between the Loop Current activity and the Gulf Stream Extension—an area characterized by strong air–sea interactions and which is key to the cyclogenesis in the North Atlantic.

Acknowledgments. Constructive comments by two anonymous reviewers are gratefully acknowledged. JH, AB, and BS acknowledge funding from the NERC project MESO-CLIP (NE/K005928/1) and from the NERC RAPID-AMOC project DYNAMOC (NE/M005097/1). AB, BS, and AC also acknowledge funding from the NERC project ACSIS (NE/N018044/1). This work used the ARCHER U.K. National Supercomputing Service (<http://www.archer.ac.uk>) and is a contribution to the DRAKKAR project (<https://www.drakkar-ocean.eu>).

REFERENCES

- Anderson, D., and R. Corry, 1985: Ocean response to low frequency wind forcing with application to the seasonal variation in the Florida Straits–Gulf Stream transport. *Prog. Oceanogr.*, **14**, 7–40, [https://doi.org/10.1016/0079-6611\(85\)90003-5](https://doi.org/10.1016/0079-6611(85)90003-5).
- Antonov, J., R. Locarnini, T. Boyer, A. Mishonov, and H. Garcia, 2006: *Salinity*. Vol. 2, *World Ocean Atlas 2005*, NOAA Atlas NESDIS 62, 182 pp.
- Atkinson, C., H. Bryden, J. J.-M. Hirschi, and T. Kanzow, 2010: On the seasonal cycles and variability of Florida Straits, Ekman and Sverdrup transports at 26°N in the Atlantic Ocean. *Ocean Sci.*, **6**, 837–859, <https://doi.org/10.5194/os-6-837-2010>.
- Baringer, M. O., and J. C. Larsen, 2001: Sixteen years of Florida Current transport. *Geophys. Res. Lett.*, **28**, 3179–3182, <https://doi.org/10.1029/2001GL013246>.
- Biastoch, A., C. W. Böning, and J. R. E. Lutjeharms, 2008: Agulhas leakage dynamics affects decadal variability in Atlantic overturning circulation. *Nature*, **456**, 489–492, <https://doi.org/10.1038/nature07426>.
- Blaker, A. T., J. J.-M. Hirschi, G. McCarthy, B. Sinha, S. Taws, R. Marsh, A. Coward, and B. de Cuevas, 2015: Historical analogues of the recent extreme minima observed in the Atlantic meridional overturning circulation at 26°N. *Climate Dyn.*, **44**, 457–473, <https://doi.org/10.1007/s00382-014-2274-6>.
- Brodeau, L., B. Barnier, A.-M. Treguier, T. Penduff, and S. Gulev, 2010: An ERA40-based atmospheric forcing for global ocean circulation models. *Ocean Modell.*, **31**, 88–104, <https://doi.org/10.1016/j.ocemod.2009.10.005>.
- Cipollini, P., F. M. Calafat, S. Jevrejeva, A. Melet, and P. Prandi, 2017: Monitoring sea level in the coastal zone with satellite altimetry and tide gauges. *Surv. Geophys.*, **38**, 33–57, <https://doi.org/10.1007/s10712-016-9392-0>.
- Clément, L., E. Frajka-Williams, Z. Szuts, and S. Cunningham, 2014: Vertical structure of eddies and Rossby waves, and their effect on the Atlantic meridional overturning circulation at 26.5°N. *J. Geophys. Res. Oceans*, **119**, 6479–6498, <https://doi.org/10.1002/2014JC010146>.
- , —, K. Sheen, J. Brearley, and A. N. Garabato, 2016: Generation of internal waves by eddies impinging on the

- western boundary of the North Atlantic. *J. Phys. Oceanogr.*, **46**, 1067–1079, <https://doi.org/10.1175/JPO-D-14-0241.1>.
- Cunningham, S. A., and Coauthors, 2007: Temporal variability of the Atlantic Meridional Overturning Circulation at 26.5°N. *Science*, **317**, 935–938, <https://doi.org/10.1126/science.1141304>.
- de Ruijter, W. P., P. J. van Leeuwen, and J. R. Lutjeharms, 1999: Generation and evolution of Natal Pulses: Solitary meanders in the Agulhas Current. *J. Phys. Oceanogr.*, **29**, 3043–3055, [https://doi.org/10.1175/1520-0485\(1999\)029<3043:GAEONP>2.0.CO;2](https://doi.org/10.1175/1520-0485(1999)029<3043:GAEONP>2.0.CO;2).
- DiNezio, P. N., L. J. Gramer, W. E. Johns, C. S. Meinen, and M. O. Baringer, 2009: Observed interannual variability of the Florida Current: Wind forcing and the North Atlantic Oscillation. *J. Phys. Oceanogr.*, **39**, 721–736, <https://doi.org/10.1175/2008JPO4001.1>.
- Donohue, K. A., D. Watts, P. Hamilton, R. Leben, M. Kennelly, and A. Lugo-Fernández, 2016a: Gulf of Mexico loop current path variability. *Dyn. Atmos. Oceans*, **76**, 174–194, <https://doi.org/10.1016/j.dynatmoce.2015.12.003>.
- , —, —, —, and —, 2016b: Loop current eddy formation and baroclinic instability. *Dyn. Atmos. Oceans*, **76**, 195–216, <https://doi.org/10.1016/j.dynatmoce.2016.01.004>.
- Dubranna, J., P. Pérez-Brunius, M. López, and J. Candela, 2011: Circulation over the continental shelf of the western and southwestern Gulf of Mexico. *J. Geophys. Res.*, **116**, C08009, <https://doi.org/10.1029/2011JC007007>.
- Duchez, A., E. Frajka-Williams, N. Castro, J. Hirschi, and A. Coward, 2014: Seasonal to interannual variability in density around the canary islands and their influence on the Atlantic meridional overturning circulation at 26.5°N. *J. Geophys. Res. Oceans*, **119**, 1843–1860, <https://doi.org/10.1002/2013JC009416>.
- Frajka-Williams, E., W. Johns, C. Meinen, L. Beal, and S. Cunningham, 2013: Eddy impacts on the Florida Current. *Geophys. Res. Lett.*, **40**, 349–353, <https://doi.org/10.1002/grl.50115>.
- Grégorio, S., T. Penduff, G. Sérazin, J.-M. Molines, B. Barnier, and J. Hirschi, 2015: Intrinsic variability of the Atlantic meridional overturning circulation at interannual-to-multidecadal time scales. *J. Phys. Oceanogr.*, **45**, 1929–1946, <https://doi.org/10.1175/JPO-D-14-0163.1>.
- Hamilton, P., J. C. Larsen, K. D. Leaman, T. N. Lee, and E. Waddell, 2005: Transports through the Straits of Florida. *J. Phys. Oceanogr.*, **35**, 308–322, <https://doi.org/10.1175/JPO-2688.1>.
- Hirschi, J. J.-M., P. D. Killworth, and J. R. Blundell, 2007: Subannual, seasonal and interannual variability of the North Atlantic meridional overturning circulation. *J. Phys. Oceanogr.*, **37**, 1246–1265, <https://doi.org/10.1175/JPO3049.1>.
- , A. T. Blaker, B. Sinha, A. Coward, B. de Cuevas, S. Alderson, and G. Madec, 2013: Chaotic variability of the meridional overturning circulation on subannual to interannual timescales. *Ocean Sci.*, **9**, 805–823, <https://doi.org/10.5194/os-9-805-2013>.
- Johns, W. E., and Coauthors, 2011: Continuous, array-based estimates of Atlantic Ocean heat transport at 26.5°N. *J. Climate*, **24**, 2429–2449, <https://doi.org/10.1175/2010JCLI3997.1>.
- Jouanno, J., J. Ochoa, E. Pallàs-Sanz, J. Sheinbaum, F. Andrade-Canto, J. Candela, and J.-M. Molines, 2016: Loop Current frontal eddies: Formation along the Campeche Bank and impact of coastally trapped waves. *J. Phys. Oceanogr.*, **46**, 3339–3363, <https://doi.org/10.1175/JPO-D-16-0052.1>.
- Kanzow, T., H. L. Johnson, D. Marshall, S. A. Cunningham, J. J.-M. Hirschi, A. Mujahid, H. L. Bryden, and W. E. Johns, 2009: Basin-wide integrated volume transports in an eddy-filled ocean. *J. Phys. Oceanogr.*, **39**, 3091–3110, <https://doi.org/10.1175/2009JPO4185.1>.
- Larsen, J., and F. T. Smith, 1992: Transport and heat flux of the Florida current at 27°N derived from cross-stream voltages and profiling data: Theory and observations. *Philos. Trans. Roy. Soc. London*, **338**, 169–236, <https://doi.org/10.1098/rsta.1992.0007>.
- Leroux, S., T. Penduff, L. Bessières, J.-M. Molines, J.-M. Brankart, G. Sérazin, B. Barnier, and L. Terray, 2018: Intrinsic and atmospheric forced variability of the AMOC: Insights from a large-ensemble ocean hindcast. *J. Climate*, **31**, 1183–1203, <https://doi.org/10.1175/JCLI-D-17-0168.1>.
- Lin, Y., R. J. Greatbatch, and J. Sheng, 2010: The influence of Gulf of Mexico Loop Current intrusion on the transport of the Florida Current. *Ocean Dyn.*, **60**, 1075–1084, <https://doi.org/10.1007/s10236-010-0308-0>.
- Liu, Z., L. Wu, and E. Bayler, 1999: Rossby wave–coastal Kelvin wave interaction in the extratropics. Part I: Low-frequency adjustment in a closed basin. *J. Phys. Oceanogr.*, **29**, 2382–2404, [https://doi.org/10.1175/1520-0485\(1999\)029<2382:RWCKWI>2.0.CO;2](https://doi.org/10.1175/1520-0485(1999)029<2382:RWCKWI>2.0.CO;2).
- Locarnini, R., A. Mishonov, J. Antonov, T. Boyer, H. Garcia, O. Baranova, M. Zweng, and D. Johnson, 2006: *Temperature*. Vol. 1, *World Ocean Atlas 2005*, NOAA Atlas NESDIS 61, 182 pp.
- Lutjeharms, J., and H. Roberts, 1988: The Natal pulse: An extreme transient on the Agulhas Current. *J. Geophys. Res.*, **93**, 631–645, <https://doi.org/10.1029/JC093iC01p00631>.
- Madec, G., 2008: NEMO ocean engine. Note du Pole de modelisation 27, Institut Pierre-Simon Laplace, 209 pp.
- , and M. Imbard, 1996: A global ocean mesh to overcome the North Pole singularity. *Climate Dyn.*, **12**, 381–388, <https://doi.org/10.1007/BF00211684>.
- Marzocchi, A., J. J.-M. Hirschi, N. P. Holliday, S. A. Cunningham, A. T. Blaker, and A. C. Coward, 2015: The North Atlantic subpolar circulation in an eddy-resolving global ocean model. *J. Mar. Syst.*, **142**, 126–143, <https://doi.org/10.1016/j.jmarsys.2014.10.007>.
- McCarthy, G., and Coauthors, 2012: Observed interannual variability of the Atlantic meridional overturning circulation at 26.5°N. *Geophys. Res. Lett.*, **39**, L19609, <https://doi.org/10.1029/2012GL052933>.
- Meinen, C. S., M. O. Baringer, and R. F. Garcia, 2010: Florida Current transport variability: An analysis of annual and longer-period signals. *Deep-Sea Res. I*, **57**, 835–846, <https://doi.org/10.1016/j.dsr.2010.04.001>.
- Mildner, T. C., C. Eden, and L. Czeschel, 2013: Revisiting the relationship between Loop Current rings and Florida Current transport variability. *J. Geophys. Res. Oceans*, **118**, 6648–6657, <https://doi.org/10.1002/2013JC009109>.
- Niiler, P. P., and W. S. Richardson, 1973: Seasonal variability of the Florida Current. *J. Mar. Res.*, **31**, 144–167.
- Oey, L.-Y., H.-C. Lee, and W. J. Schmitz, 2003: Effects of winds and Caribbean eddies on the frequency of Loop Current eddy shedding: A numerical model study. *J. Geophys. Res. Oceans*, **108**, 6425–6436, <https://doi.org/10.1029/2002JC001698>.
- , T. Ezer, and H.-C. Lee, 2005: Loop Current, rings and related circulation in the Gulf of Mexico: A review of numerical models and future challenges. *Circulation in the Gulf of Mexico: Observations and Models*, *Geophys. Monogr.*, Vol. 161, Amer. Geophys. Union, 31–56.

- Penduff, T., M. Juza, W. K. Dewar, B. Barnier, J. Zika, A.-M. Treguier, J.-M. Molines, and N. Audiffren, 2011: Sea-level expression of intrinsic and forced ocean variabilities at interannual timescales. *J. Climate*, **24**, 5652–5670, <https://doi.org/10.1175/JCLI-D-11-00077.1>.
- Putrasahan, D., I. Kamenkovich, M. Le Hénaff, and B. Kirtman, 2017: Importance of ocean mesoscale variability for air-sea interactions in the Gulf of Mexico. *Geophys. Res. Lett.*, **44**, 6352–6362, <https://doi.org/10.1002/2017GL072884>.
- Sanchez-Franks, A., S. Hameed, and R. E. Wilson, 2016: The Icelandic Low as a predictor of the Gulf Stream north wall position. *J. Phys. Oceanogr.*, **46**, 817–826, <https://doi.org/10.1175/JPO-D-14-0244.1>.
- Sheinbaum, J., G. Athié, J. Candela, J. Ochoa, and A. Romero-Arteaga, 2016: Structure and variability of the Yucatan channel and shelf break of the Yucatan channel and Campeche bank. *Dyn. Atmos. Oceans*, **76**, 217–239, <https://doi.org/10.1016/j.dynatmoce.2016.08.001>.
- Sinha, B., B. Topliss, A. T. Blaker, and J.-M. Hirschi, 2013: A numerical model study of the effects of interannual time scale wave propagation on the predictability of the Atlantic meridional overturning circulation. *J. Geophys. Res. Oceans*, **118**, 131–146, <https://doi.org/10.1029/2012JC008334>.
- Smeed, D., and Coauthors, 2014: Observed decline of the Atlantic meridional overturning circulation 2004–2012. *Ocean Sci.*, **10**, 29–38, <https://doi.org/10.5194/os-10-29-2014>.
- Stommel, H., 1948: The westward intensification of wind-driven ocean currents. *Eos, Trans. Amer. Geophys. Union*, **29**, 202–206, <https://doi.org/10.1029/TR029i002p00202>.
- Tsugawa, M., and H. Hasumi, 2010: Generation and growth mechanism of the Natal Pulse. *J. Phys. Oceanogr.*, **40**, 1597–1612, <https://doi.org/10.1175/2010JPO4347.1>.
- van Leeuwen, P. J., W. P. Ruijter, and J. R. Lutjeharms, 2000: Natal pulses and the formation of Agulhas rings. *J. Geophys. Res.*, **105**, 6425–6436, <https://doi.org/10.1029/1999JC900196>.
- van Sebille, E., and P. J. van Leeuwen, 2007: Fast northward energy transfer in the Atlantic due to Agulhas rings. *J. Phys. Oceanogr.*, **37**, 2305–2315, <https://doi.org/10.1175/JPO3108.1>.
- Zhai, X., H. L. Johnson, and D. P. Marshall, 2010: Significant sink of ocean-eddy energy near western boundaries. *Nat. Geosci.*, **3**, 608–612, <https://doi.org/10.1038/ngeo943>.